

# LIDAR-assisted Wind Turbine Gain Scheduling Control for Load Reduction

Jie Bao, Hong Yue, William E. Leithead  
Department of Electronic and Electrical Engineering  
University of Strathclyde  
Glasgow, G1 1XW, UK  
jie.bao@strath.ac.uk; hong.yue@strath.ac.uk;  
w.leithead@strath.ac.uk

Jiqiang Wang  
Jiangsu Province Key Laboratory of Aerospace Power  
System  
Nanjing University of Aeronautics and Astronautics  
Nanjing, 210016, China  
jiqiang.wang@nuaa.edu.cn

**Abstract**—A gain-scheduled feedforward controller employing pseudo-LIDAR wind measurement is designed to augment the baseline feedback controller for wind turbine load reduction during above rated operation. The feedforward controller is firstly designed based on a linearised wind turbine model at one specific wind speed, then expanded for full above rated operational envelope with gain scheduling. The wind evolution model is established using the pseudo-LIDAR measurement data which is generated from Bladed using a designed sampling strategy. The combined feedforward and baseline control system is simulated on a 5MW industrial wind turbine model developed at Strathclyde University. Simulation results demonstrate that the gain scheduling feedforward control strategy can improve the rotor and tower load reduction performance for large wind turbines.

**Keywords**—wind turbine control; LIDAR measurement; feedforward control; gain scheduling; load reduction

## I. INTRODUCTION

### A. Background

Wind energy, as a clean and renewable resource, plays one of the main roles in today's global energy market. With the increasing installed wind power capacity over the past few years, cost of wind energy production becomes a more and more important issue in wind industry. The scale of individual wind turbine has been increasing over the years because a large machine is approved to be more cost-effective owing to its stronger ability of energy capture and higher land use efficiency. However, large wind turbines have large mechanical loads on turbine structure and components, which may cause serious fatigue damage during long-time operation. It is therefore crucial to develop control systems that can reduce loads effectively for large-scale wind turbines.

Conventional wind turbine control systems employ feedback control schemes involving PI/PID controllers [1]. The main control objectives are to maximise the energy capture in below rated operation and maintain the power output at its rated level in above rated operation. Additionally, load reduction needs to be handled carefully especially for large machines. It is always a challenging task to achieve load reduction without compromising energy capture performance.

The mechanical loads on a wind turbine are mainly caused by the interaction between the turbine and the wind field

experienced by the turbine. This includes the structural loads which are the direct impacts from the wind to the turbine structure, and the drive-train loads which are the loads that propagate down to the drive-train components [2, 3]. During the past several years, three main feedback control techniques have been developed for wind turbine load reduction. The first one is the coordinated control strategy which controls the generator torque and the blade pitch together in above rated conditions [4, 5]. The second one is to add an additional drive-train filter and a tower filter to the main feedback control loop which can damp the drive train and tower vibration, as described in [6, 7]. The third one is the individual pitch control which controls the pitch angle locally for each blade [8].

Load reduction approaches based on feedback control scheme have an inherent problem, i.e., the loads which are determined from the turbine dynamics can only be controlled after they influence the turbine. In other words, there is always a delay between the load impact and the controller response. A possible solution to this problem is to employ the incoming wind disturbance information into the control system in advance so that the controller can respond to the disturbance and thereby alleviate the induced loads timely. This method depends on direct and accurate wind measurement to estimate the disturbance.

### B. LIDAR in Wind Turbine Control

In traditional wind measurement for individual wind turbine, a wind anemometer is mounted on top of the nacelle, which measures the point wind speed when the wind field passes the turbine rotor plane. This wind speed measurement is hard to be accurate because the wind field is significantly affected by the rotating rotor blades. In the past decade, a new measurement technology, Light Detection and Ranging (LIDAR), has been developed for wind measurement, with which the wind field can be detected remotely before it reaches the turbine, therefore the preview wind information can be obtained. Moreover, LIDAR can also provide the wind profile over a spatial distribution by its scanning pattern. These benefits enable the considerations of LIDAR-assisted wind turbine control development.

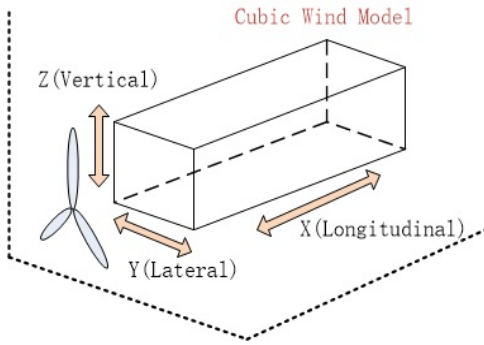


Fig. 1. LIDAR wind model in Bladed

Discussions on LIDAR principles, configurations and mounted options can be found in [9, 10], and the data analyses from LIDAR measurement can be found in [11, 12]. With these developments, LIDAR-based feedforward control has been proposed as complementary to the baseline control system so as to enhance the above rated pitch control performance. Existing methods include the use of basic feedforward schemes for collective pitch control [13–15] and individual pitch control [16], and some advanced feedforward control algorithms such as feedforward control with non-causal series expansion approximation [17], H-infinity preview control [18], adaptive control [19]. Optimisation techniques such as model predictive control (MPC) have also been investigated which includes linear methods [20, 21] and nonlinear algorithms [22]. Field testing studies have been presented for both feedforward control [23, 24] and MPC [25].

Motivated by the recent development of LIDAR in wind turbine control, in this work, a LIDAR-assisted feedforward controller is developed for nonlinear large-scale wind turbines with the aim to reduce load effectively. In our previous work [26], the controller was only designed for a linearised operating point. In this paper, the controller is further developed with gain scheduling, both the above rated condition and the transition (i.e. the region between below and above rated region) condition are considered. The rest of the paper is organised as follows. In section II, the pseudo-LIDAR data production with a designed sampling strategy is introduced. Section III gives the details on the gain-scheduling feedforward control method. The simulation studies on a 5MW machine are presented in Section IV, and conclusions are given in Section V.

## II. PSEUDO-LIDAR WIND MEASUREMENT

### A. Pseudo-LIDAR Data Preparation

As the first step of this work, measurement information of the incoming wind speed to the turbine is required. In this paper, LIDAR measurement is represented by simulated wind data, which is produced from the software Bladed.

Bladed can model a three-dimensional turbulent wind field. The cubic structure consists of a number of points that are uniformly distributed inside the cubic, as depicted in Fig. 1. Each point contains wind speed information including

the longitudinal, lateral and vertical components. To simplify the terminology, we use  $X$ ,  $Y$  and  $Z$  to denote these three components respectively. Thus, the model is defined in a 3D  $X$ - $Y$ - $Z$  coordinate system.

In the model as shown in Fig. 1, wind speed variations for the points along the  $X$  axis are regarded as the time variations of wind speed in a fixed position. Therefore, all the point wind speed time variations at the  $Y$ - $Z$  plane can be obtained by the point wind speed spatial variations along the  $X$  axis. Since the  $Y$ - $Z$  plane covers the area of the turbine rotor, this plane can be defined as the rotor plane. Consequently, all the point wind speed at the rotor plane can be obtained.

In Bladed, the wind model is generated using Veers method [27], in which the turbulence structure is isotropic. In this structure, the correlations between each point along the three components are identical and thereby one of the three components can be represented by the other two components. Based on this property, a new sampling strategy is designed to reconstruct the wind model. In previous implementation, the  $X$  axis is defined as the time axis and also the wind field incoming direction which is perpendicular to the turbine rotor plane. In the new design, the time axis is still represented by the  $X$  axis, but the wind incoming direction is selected to be defined on the  $Y$  axis. As a result, the  $X$ - $Z$  planes in the cubic structure represent the planes which are parallel to the rotor plane, as shown in Fig. 2.

In Fig. 2, the leftmost  $X$ - $Z$  plane can be defined as the rotor plane, thus the other  $X$ - $Z$  planes selected along the  $Y$  axis can be defined as the LIDAR scanning planes with different distances to the rotor plane, which can thereby provide the incoming wind profile information at different positions. Therefore, in this reconstructed sampling model, the points along the  $Y$  axis represent the positions with certain distances to the turbine rotor, and the wind speed variations in time domain is represented by the point speed along the  $X$  axis. The spatial interval between the points along the  $X$  axis is defined as the time intervals. If a set of points are selected from each  $X$ - $Z$  plane (i.e. the rotor plane and LIDAR measurement plane), the wind speed time series data for each point will be different, which is true in real world, known as the wind evolution. For this reason, the pseudo-LIDAR wind

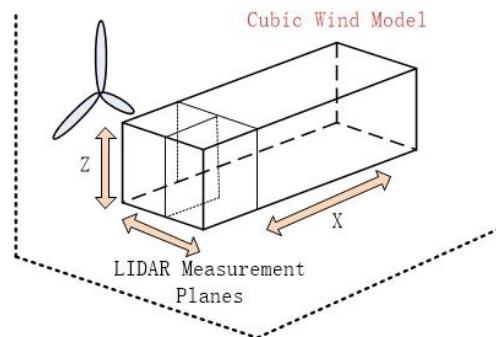


Fig. 2. Reconstructed wind model with LIDAR measurement

measurement in different positions can be established from this reconstructed model.

Using the above sampling method to create pseudo-LIDAR measurement data, eight X-Z planes are selected along the Y axis with equal distance between each other. The first plane represents the rotor plane, the other seven planes represent the LIDAR measurement planes at distances of 14.2857m, 28.5714m, 42.8571m, 57.1428m, 71.4285m, 85.7142m and 100m, respectively, from the rotor plane. The point wind speeds distributed over the plane are averaged to represent the wind speed at that plane position. In this way, the rotor wind speed data and the LIDAR measurement data can be obtained.

### B. Pseudo-LIDAR Data Analysis

In order to present the wind evolution property, correlations between rotor wind speed and each LIDAR measurement are firstly examined.

Fig. 3 and Fig. 4 illustrate the auto-spectrum of the wind speed data series for each LIDAR measurement plane and the cross-spectrum between the rotor wind speed and the other seven LIDAR wind speed series. The wind speed is generated with a mean value of 16 m/s and a turbulence intensity of 0.1 in this simulation. Auto-spectrum and cross-spectrum will be further used to apply the wind evolution during controller design.

## III. FEEDFORWARD CONTROLLER DESIGN

### A. Baseline Control System

The wind turbine model and the baseline control system used in this paper is the 5MW Supergen Exemplar wind turbine model developed at Strathclyde University. The whole system consists of five main parts, the nonlinear wind turbine model, the torque feedback controller, the pitch feedback controller, the drive-train filter and the tower filter. The torque controller maximises the energy capture in below rated operation and the pitch controller maintains the power output at its rated level above rated. Additionally, a drive-train filter and a tower filter are developed in the control system to damp the drive-train components resonance and the tower fore-aft vibration, in response to the measured generator speed and tower fore-aft acceleration. More details can be found in [28].

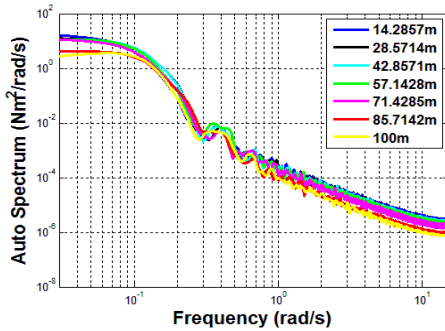


Fig. 3. Auto-spectrums for each LIDAR measurement

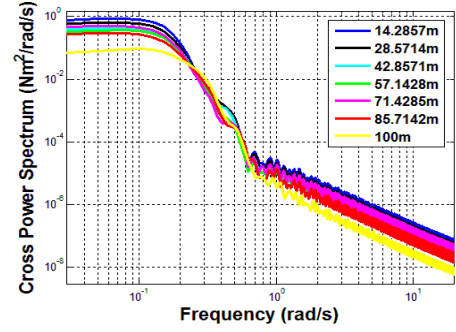


Fig. 4. Cross-spectrums between rotor and each LIDAR measurement

### B. Feedforward Controller Design

As shown in Fig. 5, a feedforward channel is added to the above baseline pitch controller to compensate the wind disturbance with the use of LIDAR measurement. In order to design the feedforward controller, the wind turbine model is firstly linearised at an above rated wind speed operating point. Fig. 6 illustrates the block diagram of such a linear control scheme. The linearised turbine model consists of two components, which are denoted by  $G_1$  and  $G_2$  in the diagram.  $G_1$  is the transfer function from the wind speed,  $V$ , to the output generator speed,  $\omega_o$ , and  $G_2$  is the transfer function from the pitch demand,  $\beta$ , to the generator speed,  $\omega_o$ . The transfer functions of the feedback pitch controller and the feedforward controller are represented by  $G_{FB}$  and  $G_{FF}$ .  $\omega_{set}$  is the generator speed setpoint.  $G_L$  denotes the measured LIDAR wind speed and  $G_E$  denotes the wind evolution process from the LIDAR detecting position to the turbine rotor. Thus, for the system shown in Fig. 6, the relationship between the input and output can be described as,

$$\omega_o = VG_E G_1 + [VG_L G_{FF} + (\omega_{set} - \omega_o) G_{FB}] G_2 \quad (1)$$

$$(1 + G_{FB} G_2) \omega_o = \omega_{set} G_{FB} G_2 - V (G_E G_1 + G_L G_{FF} G_2) \quad (2)$$

$$\omega_o = \omega_{set} \frac{G_{FB} G_2}{1 + G_{FB} G_2} + V \frac{G_E G_1 + G_L G_{FF} G_2}{1 + G_{FB} G_2} \quad (3)$$

Subsequently, to compensate the effect from the measured wind disturbance to the generator speed, the feedforward

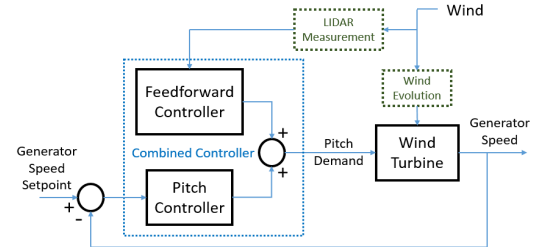


Fig. 5. Feedforward controller combined with baseline feedback controller

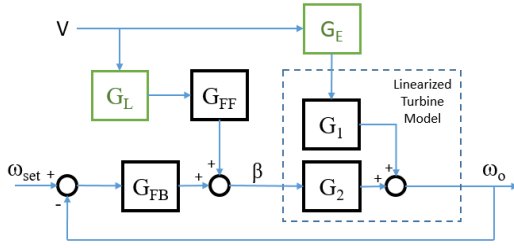


Fig. 6. Block diagram of the feedforward control system

controller is designed to make the disturbance transfer function as 0, i.e.,

$$\frac{G_E G_1 + G_L G_{FF} G_2}{1 + G_{FB} G_2} = 0 \quad (4)$$

This gives the feedforward controller

$$G_{FF} = -\frac{G_1 G_E}{G_2 G_L} \quad (5)$$

where  $G_1$  and  $G_2$  are known directly from the linearised turbine model, and the relationship between  $G_E$  and  $G_L$  can be estimated by the auto-spectrum of the LIDAR wind speed,  $S_A$ , and the cross-spectrum between the rotor wind speed and the LIDAR wind speed,  $S_C$  [24], as shown in (6).  $S_A$  and  $S_C$  can be derived from the results in section II of this paper.

$$\frac{G_E}{G_L} = \frac{S_A}{S_C} \quad (6)$$

It should be noted that the transfer function  $G_2$  contains nonminimum phase zeros (NPZ) in the right half plane. When conducting the inverse calculation, these zeros would become poles leading to an unstable system. To obtain a stable approximation, the NPZ-ignore method [29] is used to remove the NPZ zeros.

### C. Gain Scheduling

To handle the nonlinearities of the wind turbine model over the full operating range, gain scheduling is employed in developing the feedforward controller. For this turbine model, the rated wind speed is 11.55 m/s and the cut-out wind speed is 25 m/s. Therefore, we design the feedforward controller at a given speed as discussed above, and then calculate the feedforward gain for each wind speed from 12 m/s to 25 m/s with an interval of 0.5. These feedforward gains are scheduled by applying a lookup table in the system design.

## IV. SIMULATIONS AND RESULTS

To examine the performance of the proposed control strategy, simulations are implemented to the 5MW Supergen non-linear wind turbine model. The performance of the combined feedforward and baseline feedback controller is compared with that of the baseline controller only. The pitch angle demand, the out-of-plane rotor torque, the tower fore-aft acceleration and the generated power are observed to evaluate the control performance on the pitch actuator, rotor loads, tower loads and power output, respectively. There are two groups of

simulations, one employs a 12 m/s mean wind speed which corresponds to the transition region between below and above rated operation, the other employs a 20 m/s mean wind speed which represents the high wind speed region.

### A. Transition Region

A turbulent wind with mean wind speed of 12 m/s and turbulence intensity of 0.1 is applied in simulation. The results are generated in frequency domain taking the measure of power spectral density (PSD).

In Fig. 7, a reduction in the pitch demand PSD can be observed from the results using the combined feedforward and feedback control. This means that the pitch angle demand variations are reduced, which is positive for energy saving and lifetime extension of the pitch actuator. With the proposed method, the deduction of the out-of-plane rotor torque and the tower fore-aft acceleration PSD can be observed in Fig. 8 and Fig. 9, which demonstrates the improvement on rotor and tower loads reduction. Next, as a significant assessment of wind turbine performance, the effect on the power output is also examined. As shown in the frequency domain results in Fig. reffig10, the generated power is not much affected.

### B. High Wind Speed Region

A turbulent wind with mean wind speed of 20 m/s and turbulence intensity of 0.1 is applied to represent a high speed. Similar to the simulations in the transition region, results in the high wind speed region, shown in Figs. 11 - 13, also demonstrate the reduction on the pitch variations, the rotor loads and the tower loads when using the proposed method. The performance improvement of tower loads reduction is not as obvious as in the transition region, but the improvement can still be observed. And finally, Fig. 14 shows that the power generation performance is still maintained when the feedforward controller is added to the system. This again suggests that when employing the proposed method to reduce wind turbine loads, the power production performance is not compromised.

## V. CONCLUSIONS

In this paper, a gain scheduled feedforward controller based on LIDAR measurement is designed and applied to complement the baseline feedback controller. Pseudo-LIDAR wind

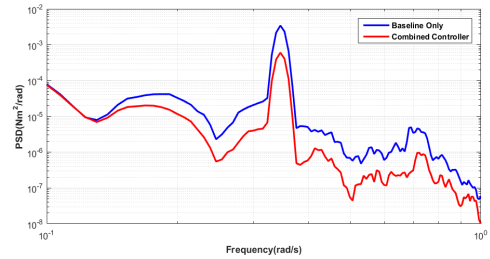


Fig. 7. Comparison of the pitch demand PSD (mean wind 12 m/s, blue line represents the baseline controller, red line represents the combined feedforward and feedback controller)

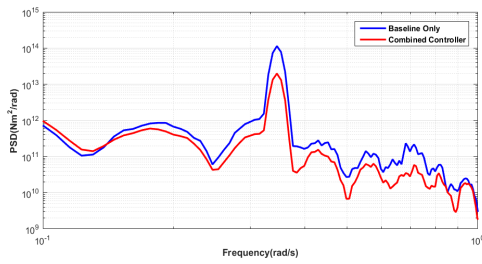


Fig. 8. Comparison of the rotor torque PSD (mean wind 12 m/s)

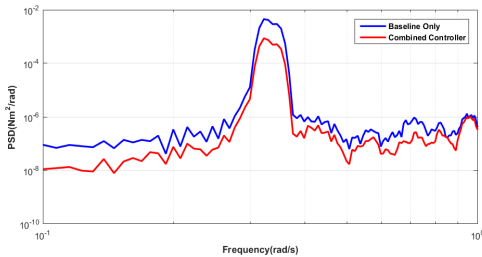


Fig. 9. Comparison of the tower acceleration PSD (mean wind 12 m/s)

measurement is generated using Bladed with a designed sampling strategy. The performance of the combined feedforward and baseline feedback control system is compared with the baseline feedback control. Simulation studies are implemented for both the transition region and the high wind speed region.

The baseline control system has its own components for load reduction purpose, which are the drive-train filter and the tower filter. However, simulation results demonstrate that further load reductions on rotor and tower can be achieved with the use of the feedforward controller. These improvements could also influence the drive-train components, since the rotor loads will propagate down to the drive-train. As a result, the fatigue loads on the wind turbine could be reduced leading to an extended lifetime and a reduced maintenance cost. Moreover, the reduction on pitch variations is also achieved, which implies a less aggressive pitch actuator dynamics. Finally, it can be observed that the power generation performance is not affected by the proposed control method. Comparing with the result in high wind speed region, the combined

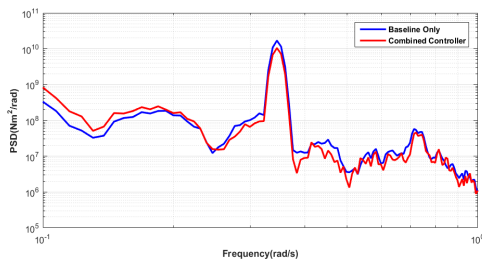


Fig. 10. Comparison of the generated power PSD (mean wind 12 m/s)

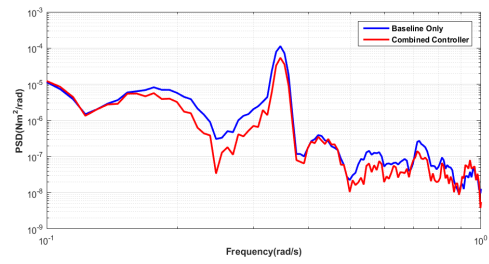


Fig. 11. Comparison of the pitch demand PSD (mean wind 20 m/s)

controller in the transition region has more clear improvements on pitch dynamics and load reduction performance, but makes more influences on the power output. The feedforward control algorithm needs to be further investigated to drive its full potential. The control performance in extreme load conditions will also be investigated in future studies.

## REFERENCES

- [1] E. Bossanyi, "The design of closed loop controllers for wind turbines," *Wind Energy*, vol. 3, no. 3, pp. 149–163, 2000.
- [2] W. Leithead and B. Connor, "Control of variable speed wind turbines: design task," *Int. J. Control*, vol. 73, no. 13, pp. 1189–1212, 2000.
- [3] F. D. Bianchi, H. D. Battista, and R. J. Mantz, *Wind Turbine Control Systems: Principles, Modelling and Gain Scheduling Design. Advances in Industrial Control*. Springer, 2007.
- [4] W. Leithead, S. Dominguez, and C. Spruce, "Analysis of tower/blade interaction in the cancellation of the tower fore-aft mode via control," in *Proc. EWEC 2004, London, UK, 2004*.
- [5] W. E. Leithead and S. Dominguez, "Coordinated control design for wind turbine control systems," in *Proc. EWEC, Athens, Greece*, vol. 27, 2006.
- [6] E. Bossanyi, "Wind turbine control for load reduction," *Wind Energy*, vol. 6, no. 3, pp. 229–244, 2003.
- [7] W. Leithead and S. Dominguez, "Controller design for the cancellation of the tower fore-aft mode in a wind turbine," in *Proc. 44th IEEE Conf. Decision and Control*, 2005, pp. 1276–1281.

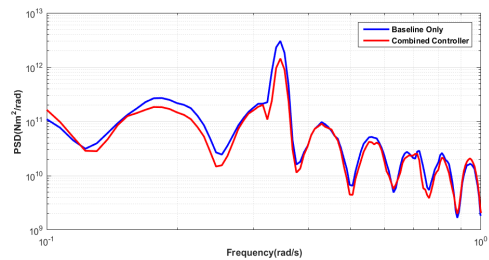


Fig. 12. Comparison of the rotor torque PSD (mean wind 20 m/s)

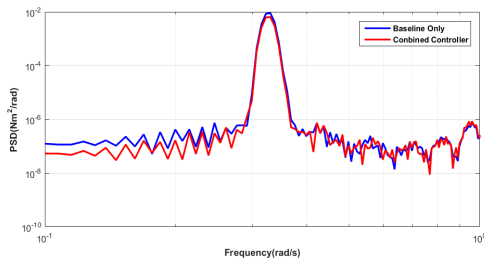


Fig. 13. Comparison of the tower acceleration PSD (mean wind 20 m/s)

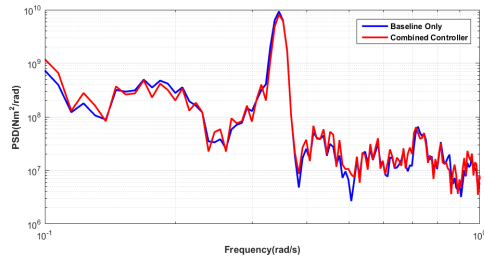


Fig. 14. Comparison of the generated power PSD (mean wind 20 m/s)

- [8] E. Bossanyi, "Individual blade pitch control for load reduction," *Wind Energy*, vol. 6, no. 2, pp. 119–128, 2003.
- [9] M. Harris, M. Hand, and A. Wright, "Lidar for turbine control," *NREL, Golden, CO, Report No. NREL/TP-500-39154*, 2006.
- [10] T. Mikkelsen, K. H. Hansen, N. Angelou, M. Sjöholm, M. Harris, P. Hadley, R. Scullion, G. Ellis, and G. Vives, "Lidar wind speed measurements from a rotating spinner," in *Proc. EWEC 2010, Warsaw, Poland*, 2010.
- [11] M. Sjöholm, T. Mikkelsen, J. Mann, K. Enevoldsen, and M. Courtney, "Spatial averaging-effects on turbulence measured by a continuous-wave coherent lidar," *Meteorologische Zeitschrift*, vol. 18, no. 3, pp. 281–287, 2009.
- [12] M. Sjöholm, T. Mikkelsen, L. Kristensen, J. Mann, and P. Kirkegaard, "Spectral analysis of wind turbulence measured by a doppler lidar for velocity fine structure and coherence studies," *Detailed Program*, 2010.
- [13] D. Schlipf and M. Kühn, "Prospects of a collective pitch control by means of predictive disturbance compensation assisted by wind speed measurements," in *Proc. GWEC DEWEC 2008, Bremen, Germany*, 2008.
- [14] D. Schlipf, E. Bossanyi, C. E. Carcangiu, T. Fischer, T. Maul, and M. Rossetti, "Lidar assisted collective pitch control," *UpWind Deliverable D5.1.3, Stuttgart, Germany*, 2011.
- [15] J. Laks, L. Pao, and A. Wright, "Combined feedforward/feedback control of wind turbines to reduce blade flap bending moments," in *Proc. 47th AIAA Meet., Orlando, FL, AIAA-2009-687*, 2009.
- [16] F. Dunne, D. Schlipf, L. Y. Pao, A. D. Wright, B. Jonkman, N. Kelley, and E. Simley, "Comparison of two independent lidar-based pitch control designs," *50th AIAA Meet., Nashville, Tennessee, USA*, 2012.
- [17] F. Dunne, L. Y. Pao, A. D. Wright, B. Jonkman, and N. Kelley, "Adding feedforward blade pitch control to standard feedback controllers for load mitigation in wind turbines," *Mechatronics*, vol. 21, no. 4, pp. 682–690, 2011.
- [18] J. Laks, L. Pao, A. Wright, N. Kelley, and B. Jonkman, "The use of preview wind measurements for blade pitch control," *Mechatronics*, vol. 21, no. 4, pp. 668–681, 2011.
- [19] N. Wang, K. E. Johnson, and A. D. Wright, "Fx-rls-based feedforward control for lidar-enabled wind turbine load mitigation," *IEEE Trans. Control Syst. Tech.*, vol. 20, no. 5, pp. 1212–1222, 2012.
- [20] J. Laks, L. Y. Pao, E. Simley, A. Wright, N. Kelley, and B. Jonkman, "Model predictive control using preview measurements from lidar," in *Proc. 49th AIAA Meet., Orlando, FL, USA*, 2011.
- [21] D. Schlipf, L. Y. Pao, and P. W. Cheng, "Comparison of feedforward and model predictive control of wind turbines using lidar," *51st IEEE Conf. Decision & Control (CDC), Maui, Hawaii, USA*, pp. 3050–3055, 2012.
- [22] D. Schlipf, D. J. Schlipf, and M. Kühn, "Nonlinear model predictive control of wind turbines using lidar," *Wind Energy*, vol. 16, no. 7, pp. 1107–1129, 2013.
- [23] A. Scholbrock, P. Fleming, L. Fingersh, A. Wright, D. Schlipf, F. Haizmann, F. Belen *et al.*, "Field testing lidar based feed-forward controls on the nrel controls advanced research turbine," *51st AIAA Meet., Grapevine, Texas, USA*, 2013.
- [24] D. Schlipf, P. Fleming, F. Haizmann, A. Scholbrock, M. Hofsäß, A. Wright, and P. W. Cheng, "Field testing of feedforward collective pitch control on the cart2 using a nacelle-based lidar scanner," in *J. Phys. : Conf. Series*, vol. 555, no. 1, 2014, p. 012090.
- [25] F. Haizmann, D. Schlipf, S. Raach, A. Scholbrock, A. Wright, C. Slinger, J. Medley, M. Harris, E. Bossanyi, and P. W. Cheng, "Optimization of a feed-forward controller using a cw-lidar system on the cart3," in *2015 ACC, Chicago, IL, USA*, 2015, pp. 3715–3720.
- [26] J. Bao, M. Wang, H. Yue, and W. Leithead, "Pseudo-lidar data analysis and feed-forward wind turbine control design," in *IFAC Proc. Vol., 9th IFAC Symp. ADCHEM 2015*, vol. 48, no. 8, 2015, pp. 483–488.
- [27] P. S. Veers, "Three-dimensional wind simulation," Sandia National Labs., Albuquerque, NM (USA), Tech. Rep., 1988.
- [28] A.-P. Chatzopoulos, "Full envelope wind turbine controller design for power regulation and tower load reduction," Ph.D. dissertation, University of Strathclyde, 2011.
- [29] J. A. Butterworth, L. Y. Pao, and D. Y. Abramovitch, "The effect of nonminimum-phase zero locations on the performance of feedforward model-inverse control techniques in discrete-time systems," in *2008 ACC, Seattle, Washington, USA*, 2008, pp. 2696–2702.